Aust. Met. Mag. 39 (1991) 237–245

Recent developments and performance of radar wind profilers and RASS

Peter T. May
Bureau of Meteorology Research Centre, Melbourne, Australia

(Manuscript received June 1991; revised August 1991)

A review of recent progress in the development of wind profilers for both operational and research meteorology is presented. Wind profilers are having a significant impact and are coming into use in Australia. The development of a temperature sounding capability using the RASS (radio acoustic sounding system) technique will only enhance the impact. The review concludes with discussion of ongoing work in Australia.

Introduction

Wind profilers are now a key component in many research and operational programs. Their capability to measure wind profiles with very good time (20 min–1 h) and height (150–500 m) resolution throughout the troposphere and lower stratosphere is unparalleled. Developments are still taking place on a number of fronts. Analysis techniques to take advantage of the good time resolution in both single-site analyses and networks for operational forecasting are being studied. There have also been technological advances such as the development of very portable 'boundary-layer profilers' and temperature sounding with profiler resolution up to several kilometres using the RASS (radio acoustic sounding system) technique. The wind profiler is a reasonably mature technology for wind sounding, but important research is continuing on such topics as using the radars to measure drop-size distributions in precipitation (Gossard 1988) and RASS (May et al. 1990a). This review will cover the technique and recent advances, illustrated by some applications, and will conclude with a description of research being performed in Australia.

Wind profilers are Doppler radars capable of detecting the backscatter from the fluctuations in the refractive index (which is a function of temperature and humidity) of the clear air through the troposphere (see Balsley (1981) and Larsen and Rottger (1982) for reviews). Profilers are characterised by long dwell times (of the order of minutes to obtain a velocity estimate) and observing in three or five fixed beam directions, all close to the zenith (within 15°). This is in contrast to a weather radar which is continually scanning and uses dwell times of less than a second. The radial velocity of the scatterers along the radar beams is measured and the wind is estimated assuming that the wind field over the beam separation is uniform. While this can lead to errors under severe convective conditions, profilers have proved to be excellent observing platforms for the study of mesoscale systems such as fronts, jet streaks and short waves (e.g. Shapiro et al. 1984). An example, using data from the Denver 915 MHz profiler, is shown in Fig. 1. Note how the very thin region of directional shear associated with the front is resolved, although the region of large velocity shear is over a layer about one kilometre thick and two hours in duration. Another interesting feature is the quasi-periodic fluctuation (period $\sim$2 h) in wind speed ahead of the front. These have a considerable amplitude (>5 m s^{-1}) and the spatial scale corresponding to a two-hour oscillation will not be spatially resolved by any foreseeable operational network. This kind of oscillation will severely contaminate the calculation of gradient

Corresponding author address: Dr P. May, Bureau of Meteorology Research Centre, GPO Box 1289K, Melbourne, Victoria 3001, Australia

Fig. 1 Observations of a cold front using the Denver 915 MHz wind profiler. Observations are every 20 min and 150 m in height from 300 m above ground. A flag is 25 m s^{-1}, full barb 5 m s^{-1} and half barb 2.5 m s^{-1}.

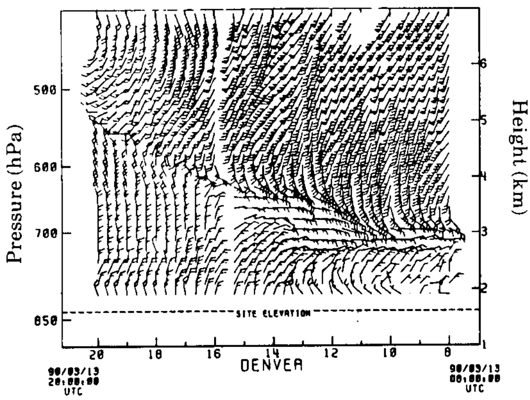

quantities such as vorticity and divergence using any observing technique, although with the profiler time resolution there is at least some hope of identifying and possibly filtering such fluctuations. Some profilers, such as the Adelaide very high frequency (VHF) radar (Vincent et al. 1987), use an alternative observing method known as the spaced antenna (SA) technique, but it has similar limitations to the technique described above (May 1990).

There have been numerous statistical comparisons between profiler and radiosonde wind estimates which have generally shown excellent agreement. The most comprehensive of these compared two years of data from a profiler and radiosondes launched from the Denver National Weather Services (NWS) site. This study showed root mean square differences of about 2.5 m s^{-1} (Weber and Wuertz 1990); very good considering that the profiler gives a volume (150 m in height) and time (15 min) average above the radar, while the radiosonde is a slantwise point measurement. With the volume and time averaging inherent with the profiler, it can be argued that profiler wind estimates should be more representative of the mean wind than radiosonde estimates. Profilers operating in the tropical Pacific are providing data to both the National Meteorological Centre (NMC) and the European Centre for Medium Range Weather Forecasts (ECMWF) (Gage et al. 1988). These data are increasing the skill of analyses in this data-sparse region.

Wind profiler types

Profilers have been built at a number of frequencies (Strauch et al. 1984). The radar equation for received backscattered power, P_r, can be written as:

$$P_r = K\, P_t\, A\, \lambda^2\, \eta\, \Delta r / r^2 \qquad \ldots 1$$

where K is a constant, P_t is the transmitted power, A is the antenna area, λ is the radar wavelength, η is the radar reflectivity, Δr is the range resolution and r is the range. The radar reflectivity from precipitation is given by:

$$\eta = C\, Z / \lambda^4 \qquad \ldots 2$$

where C is a constant and Z is the reflectivity factor (often expressed as dBZ: 10 $\log_{10}$ (Z)). For clear-air scatter from isotropic turbulence in the inertial subrange:

$$\eta = 0.38\, \lambda^{-1/3}\, C_n^2 \qquad \ldots 3$$

where C_n^2 is the turbulence structure constant. Examples of low and high power profilers are shown in Table 1. Note that the sensitivity of a profiler is proportional to the mean power multiplied by the antenna area. The strong wavelength dependence of η means that the capabilities of different frequency profilers and the relative importance of clear air and precipitation scatter differ substantially. This also impacts on their applications. Therefore, we will now discuss separately profilers operating at differing frequency bands.

50 MHz profilers

The capability of observing winds through the troposphere and lower stratosphere was first shown using high-power ionospheric radars operating near this frequency (Woodman and Guillen 1973). These systems use large antennas, about 50–100 m in diameter, and high power systems (e.g. Fukao et al. 1985) can measure winds as high as 25 km routinely, while more modest systems generally 'see' to about 15 km. Their main limitation, however, is that they have a minimum observing height of 1–2 km, which is not adequate for many meteorological applications. They have been supported by 915 MHz boundary-layer profilers, but the added complexity probably means they will not be deployed operationally. However, the 50 MHz profiler has significant research applications not feasible with profilers operating at 400 or 915 MHz. These radars can always see the backscatter from the clear air, unlike profilers at higher frequencies where the backscatter from precipitation may drown out the clear-air scatter. Thus they are one of the very few observing systems capable of directly measuring the vertical component of the wind (w) under a wide variety of conditions. This has important implications. For example, they can measure the vertical motion field around frontal regions. The vertical circulation around fronts is crucial for understanding the dynamics of fronts and these systems provide excellent tests for models. An example from the third phase of the Australian Cold Fronts Program is shown in Fig. 2. The horizontal winds above 2 km are measured by the Adelaide profiler,

Table 1. Characteristics of low and high power profilers at different frequencies.

(a) 50 MHz systems

Radar	Darwin/Saipan profiler (BMRC)	MU radar (Kyoto Univ., Japan)
Max. mean transmitter power (W)	70	8000
Antenna diam. (m)	100	100
Height resolution (m)	1000	150
Min. range (km)	~1.5	~1.2
Typical max. range (km)	~14	~25

(b) 400 MHz systems

Radar	WPL mobile radar (Wave Prop. Lab., NOAA)	NOAA prototype (UNISYS)
Max. mean transmitter power (W)	30	2000
Antenna diam. (m)	5	13
Height resolution (m)	150	375/1000
Min. range (m)	250	500
Typical max. range (km) (in clear air)	6	17

(c) 916 MHz systems

Radar	Boundary-layer profiler (Aeronomy Lab., NOAA)	WPL Denver
Max. mean transmitter power (W)	3	450
Antenna diam. (m)	2	10
Height resolution (m)	150	150/450
Min. range (m)	150	300
Typical max. range (km) (in clear air)	2	9

while the winds below 2 km and temperature observations are from six-hourly radiosondes. The temperature structure and the warm and cold conveyor-belt flows described in the conceptual model of Ryan and Wilson (1985) can be recognised with the aid of satellite observations (May et al. 1990b). Of particular interest is the vertical component and the horizontal component normal to the front. A deep upward circulation driven by low-level convergence is seen around the time of the passage of the surface front. This deep circulation is responsible for the generation of the mid-tropospheric cold dome. The circulation is a feature noted in the numerical models of Reeder and Smith (1987), but the observations show a smaller horizontal scale and are more intense. This and other cases are discussed in more detail by May et al. (1990b).

These radars have also been used for studying short time-scale wind variability associated with internal gravity waves. A key finding is that although the energy density is concentrated towards low frequencies, it is the high frequency components that are responsible for the vertical flux of horizontal momentum and the momentum flux divergence, at least near mountainous terrain (Fritts et al. 1990). The vertical flux of horizontal momentum associated with internal gravity waves has been parametrised in many large models to provide a drag on the mean flow, but this technique provides one of the few tests of these parametrisations in the real atmosphere.

When there is heavy precipitation (rainfall rates $>$ 10 mm/h), it has been observed that a second peak associated with hydrometeor scatter appears. Because we have independent measures of both the fall speed and vertical motion, as well as automatic correction for spectral broadening due to turbulence and beam width (since these are the same for clear air and precipitation), these radars may be able to measure the drop-size distribution with great sensitivity and fewer assumptions than in previous radar studies (Wakasugi et al. 1987; Gossard 1988). This kind of measurement should lead to improved estimates of rainfall from weather radar as well as better radiation transfer models for clouds, since drop-size distributions are major uncertainties in both areas. Clearly these radars will play a major role in research meteorology for some time.

Fig. 2 (a) Time-height cross-section of along-front and relative across-front wind components together with potential isotherms (K) observed with the Adelaide VHF radar. Arrow on the time axis denotes the time of arrival of the surface front. The vectors below 2 km are from rawinsonde measurements. The shaded areas are regions where the relative humidity exceeds 80% (after May et al. 1990b). (b) Time-height cross-section of vertical velocity and relative normal velocity together with potential isotherms (K). The scale at the top left is 20 cm s^{-1} and 20 m s^{-1} for the vertical and horizontal components respectively. The vectors below 2 km are rawinsonde measurements of the u component with w set to zero. The shaded areas are regions where the relative humidity exceeds 80% (after May et al. 1990b).

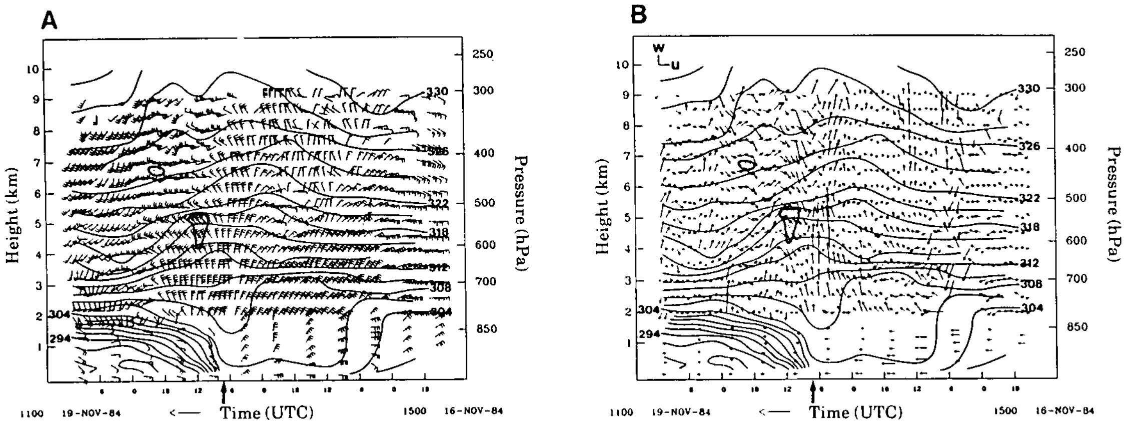

400 and 915 MHz profilers

Profilers operating at frequencies of 400 MHz and higher have somewhat different characteristics. They have more acceptable minimum observing heights, which may be as low as 200 m, and the prototype for the NOAA profiler network has routinely observed winds to greater than 15 km above ground. Even a very low-power mobile 404 MHz profiler (Moran et al. 1989) routinely sees above 6 km, which is adequate for many applications. Even quite powerful radars operating at around 915 MHz are limited to a maximum height of about 10 km (Strauch et al. 1984). This is most likely because the inner scale of turbulence becomes less than half a radar wavelength at greater heights, so the fluctuations in radar refractive index are highly damped. A small inner scale is also presumably why 10 cm weather radars are mostly limited to the boundary layer for scatter from the clear air. A significant difference compared with 50 MHz profilers is that when there is precipitation, the shorter wavelength means that the precipitation echo is many orders of magnitude greater than the clear air. This means that they cannot always measure the vertical component of the wind; instead they measure the fall speed of the precipitation. This does not, however, greatly affect the accuracy of the horizontal wind estimates (Wuertz et al. 1988). In this sense they can be regarded as supplying similar data as a radiosonde, but with more representative estimates and much better time resolution.

A number of very low power 915 MHz profilers, capable of measuring winds continuously up to about 2–3 km, have been built. These initially were designed to support 50 MHz profilers, but have been used in a number of experiments, for example in looking at flows in complex terrain. They are very useful for these and other experiments studying small-scale phenomena since the profilers are small and easily deployed.

Networks

There have been a number of studies devoted to developing single-station diagnostics using profiler-derived winds. For example Nieman and Shapiro (1989) used geostrophic methods to estimate temperature gradients and temperature advection from profiler data in regions where fronts had little curvature and were not evolving rapidly. Zamora et al. (1987) used line integral methods to obtain three station estimates of vorticity, divergence and deformation around fronts and jet-streaks. They were also able to diagnose the ageostrophic wind component in some cases. As noted earlier, profilers have been used to document fronts and jet streaks (e.g. Rottger 1979; Shapiro et al. 1984), and operationally to look at developments between the synoptic observing times (Beckman 1990). However, it is clear that many of the major benefits for operational and research meteorology will lie in the deployment of networks. NMC and ECMWF are assimilating data from the profiler network in the tropical Pacific area with a significant impact (Gage et al. 1988). With the first large network in the process of being deployed in central USA, the studies so far have been theoretical and observing system simulation experiments (OSSEs). Work by Kuo and Guo (1989) has shown that the deployment of a profiler network should have a significant positive impact on short-term forecasts mainly within the region of the network. However, the impact would be significantly enhanced by temperature measurements of comparable resolution. Until recently most remotely-sensed temperature measurements have suffered from poor height resolution. This led to efforts to extract temperature fields from profiler wind measurements using the dynamical equations (Kuo et al. 1987; Gal-Chen 1988). These approaches met with some success. In fact, the retrieval accuracy in the OSSEs was close to radiosonde accuracy on the average, but the largest errors occurred in the boundary layer and regions of strong vertical motion and dynamical forcing: precisely where the measurements are most needed. This leads us to recent developments using the RASS technique.

RASS

The RASS technique holds the promise of obtaining temperature measurements with a precision of better than a degree with profiler-type time and height resolutions, albeit over a more limited height range. RASS combines a high-power acoustic source, to create fluctuations in air density, and a clear air radar (wind profiler). The system utilises the radar backscatter from the acoustic density fluctuations to measure the speed of sound, and hence the virtual temperature (see Peters et al. (1983) and May et al. (1990a) for a comprehensive description of the technique). The concept dates back to 1960 (Fetter 1961; Atlas 1962) and was first implemented in the early 1970s (North et al. 1973). The early systems used pulsed acoustic sources and simple continuous wave (CW) radars and hence could obtain very fine height resolution, but were generally limited to observing below about 1 km. Applications included pollution monitoring and boundary-layer studies (e.g. Bonino et al. 1981). These systems required both that the acoustic wavelength be half the radar wavelength (Bragg matched) and the focussing effect of the quasi-spherical acoustic waves. As the wind displaced the sound waves the return signal rapidly diminished. However, a sensitive wind profiler can use the fringes of the backscattered energy caused by turbulent distortion of the acoustic waves. Therefore wind is much less of a problem and the height coverage is greatly increased (May et al. 1988). Success with RASS using a very high power profiler and sophisticated beam-swinging techniques resulted in temperature measurements to 20 km (Matuura et al. 1985). This in turn led to a simple form of profiler/RASS just using the vertical radar beam. Wind displacing the acoustic waves is still the limitation for 50 MHz profilers (maximum altitude 5–10 km), but acoustic attenuation is the limiting factor for 400 MHz (3–5 km) and 915 MHz (1.5–2.5 km) profilers (May et al. 1988). The attenuation is temperature and humidity-dependent with the worst conditions occurring with cool temperatures (~0°C) and low humidities.

Comparisons with over 50 radiosonde ascents in both summer and winter at Denver have shown that the present accuracy obtained with the profiler/RASS is about 1°C, comparable to radiosonde accuracy (May et al. 1989). Furthermore, it was shown that the main error was due to the vertical wind w which is additive to the measured sound speed. Now w can be measured with a profiler (at least in non-precipitating conditions) simultaneously with the RASS observation. The reason why this has not been done so far is that the profilers used had very old computer systems that lacked sufficient memory. This is now being corrected and it may be possible to obtain measurements with an accuracy of better than 0.5°C, limited by such effects as the horizontal wind and the statistical errors of the Doppler shift measurements.

The combined profiler/RASS has already been used in a number of studies. For example, Nieman et al. (1991) have studied an Arctic front which passed Denver bringing record low temperatures. The system observed temperature inversions of greater than 20°C in 150 m at an altitude of 1 km above ground. These observations were consistent with local observations and the regional radiosonde network. Figure 3 is a recent case showing the passage of a mid-level baroclinic wave associated with a polar maritime air mass over Denver. This observation combines surface measurements, profiler winds, 915 MHz RASS (up to 2 km), and 50 MHz RASS (2–6 km) where the hydrostatically calculated pressure versus height has been used to calculate the virtual potential temperature (θ_v). The front on the leading edge can be clearly identified in both the θ_v and wind fields, as can the baroclinic zone associated with the jet streak on the back side of the wave. The stable region above 450 hPa observed

Fig. 3 Time-height cross-section of a baroclinic wave observed with the Denver 915 MHz profiler (winds)/RASS (below 2 km) and Platteville 50 MHz RASS (2–6 km). The contours are of θ_v.

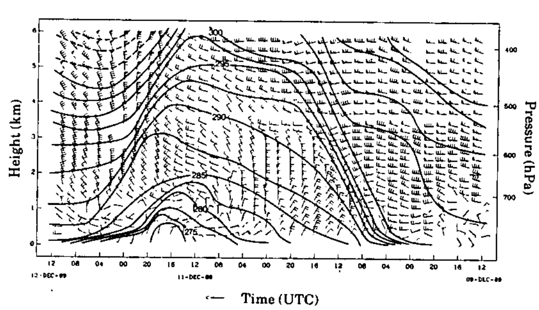

from about 1800 UTC on December 10 to 1200 UTC on December 11 corresponds to the tropopause identified by radiosondes. These data also allow the measurement of the bulk Richardson number, which has a minimum along the frontal zones, and (with a time to space conversion) the isentropic potential vorticity (IPV). Stratospheric values of IPV were observed associated with the jet streak indicating the intrusion of stratospheric air. This is all consistent with the conceptual model of such systems (e.g. Keyser and Shapiro 1986).

It is clear that the limited height coverage of RASS means that it must be supplemented with additional data for adequate profiling. Work is continuing on combining the RASS with satellite temperature profiles above the RASS coverage. This is a synergistic relation because the RASS obtains the benefits of extended height coverage, and will provide better initial guess fields and boundary conditions for the satellite retrievals (Schroeder et al. 1991). The dynamic retrieval techniques discussed earlier may also be powerful tools to expand the impact of RASS. A network of profilers with RASS will be a major source of data for improving numerical prediction models.

Australian wind profilers

There are currently three 50 MHz wind profilers being operated by Australian groups and they all offer unique research opportunities. These radars are near Adelaide (University of Adelaide), Darwin (BMRC) and Saipan (BMRC). The Adelaide profiler is uniquely situated because of its location upwind of any significant mountain range. All the other 50 MHz profilers in the mid-latitudes except one are located in or near large mountains. This means that vertical wind motions measured by these other radars are strongly contaminated by lee waves and associated turbulence. The Adelaide system is ideally located to study such features as the vertical circulations around fronts and the generation of internal gravity waves by fronts. These may have a significant impact for research on fronts and gravity waves which are responsible for considerable vertical transport of momentum.

The other two profilers are located in tropical regions. The Darwin site is a major research facility and includes Doppler weather radars and an extensive mesoscale network of surface stations. The combination of the profiler and Doppler weather radar is quite unique, and potentially very exciting. It offers numerous opportunities to monitor the environment around storms, vertical motions within storms and cloud studies. This, together with the large range of storm types observed at Darwin (Keenan and Carbone 1989), makes it an important facility. It is also one of the ground truth sites for the Tropical Rainfall Measuring Mission (TRMM).

The second BMRC profiler is located in Saipan (15° 7′ N, 145° 43′ E), in the tropical northwest Pacific. This radar was deployed as part of a network of profilers, ships and radiosondes for the Tropical Cyclone Motion Experiment (TCM-90) during August and September 1990 (Elsberry 1990). This experiment aims to study the interaction between tropical storms and the large-scale environment. The profiler is also ideally placed for studies on rainbands associated with tropical storms and to supply high temporal resolution data to support studies of storm genesis.

These radars are all research facilities, but both the Adelaide and Darwin profilers also provide data in real time for the Bureau of Meteorology regional offices. There is also a 915 MHz boundary-layer profiler used operationally at Mt Isa to support air pollution monitoring. Although an Australian network of profilers is several years away, these systems will contribute significantly both to research and operational meteorology in Australia. These profilers, used in concert with other data sources, have the potential to significantly improve the understanding of weather events.

As an example of this synthesis, a squall line observed recently in Darwin is shown in Figs 4 to 7. The weather radar reflectivity plots show a well-defined, almost classical, squall line approaching Darwin from the east. There was also a number of small isolated cells developing ahead of the squall. The leading edge of the squall contained reflectivity centres corresponding to rainfall rates in excess of 40 mm/h. There was a well-defined region of decreased radar reflectivity immediately behind the convective line and an extensive region of trailing stratiform rain extending over 100 km behind the squall. The trailing stratiform region was increasing in area, possibly in response to the upper level westerlies of 7–10 m s^{-1}, as the squall crossed Darwin. This was at around 1 am local time, and gusts of 22 m s^{-1} were recorded at Darwin Airport at 1:15 am. The leading edge of strong convective activity was observed to bow outwards as the line crossed Darwin. The squall began to dissipate after about 4 am, leaving a large region of trailing stratiform cloud. The profiler recorded winds in excess of 20 m s^{-1}, averaged over an hour, at the time of the squall line. The easterly flow at about 3 km altitude was greater than 20 m s^{-1} in the hour after the squall passage, consistent with an inflow jet into the trailing stratiform region. The magnitude of the gusts measured at the airport fits well with the downward transport of momentum associated with the storm passage. Furthermore, the bowing and acceleration of the line in the northern half of the squall was consistent with the strong inflow behind the squall observed by the profiler. The

Fig. 4 Darwin weather radar displays of reflectivity associated with the squall line at (a) 0000 CST, (b) 0130 CST and (c) 0330 CST on 11 November 1990.

(a)

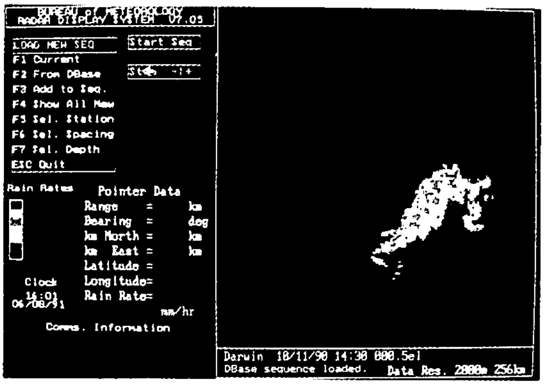

(b)

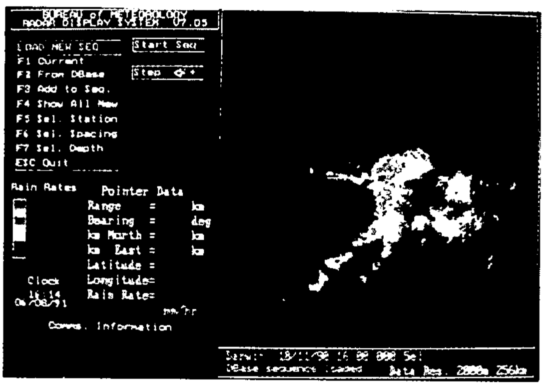

(c)

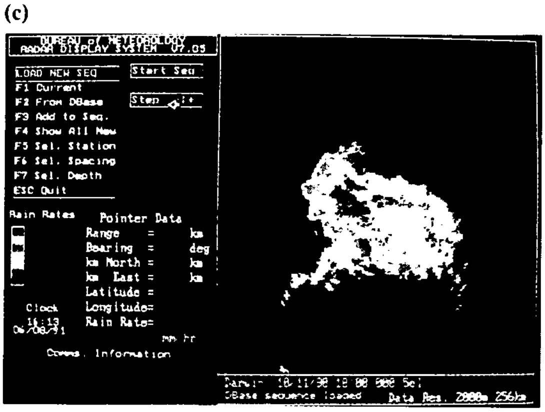

profiler also revealed a significant amount of mesoscale structure in the wind field. For example, note the southerly winds between 8 and 10 km increase in magnitude until the squall line passage, and the abrupt change in wind direction to southwesterlies.

The measured vertical motions (with the effect of the precipitation echoes removed) averaged over 30-minute periods are shown in Fig. 6. This reveals a disorganised pattern ahead of the squall. The large motions between 0000 and 0100 CST are associated with an isolated cell (~0015) and the convective line (~0100). The raw data revealed that two main updrafts (one associated with the cell and the second with the squall) passed over the radar, each with vertical velocities in excess of 5 m s^{-1} averaged over 90 seconds. The stratiform region between 0100 and 0700 clearly reveals the mesoscale downdraft below the freezing level (induced by water loading, ice melting and evaporation) and the mesoscale updraft above the freezing level. The updraft is relatively shallow, with weak subsidence above 9 km. The magnitude of the mesoscale vertical motion is about 0.25–0.5 m s^{-1}. The mesoscale circulation stops abruptly at the rear of the stratiform region. This is apparently followed by an internal gravity wave.

Fig. 5 Darwin wind profiler observations of the hourly averaged horizontal wind. The surface winds are taken from the Darwin Airport anemometer trace. The arrival of the squall is marked by the arrow.

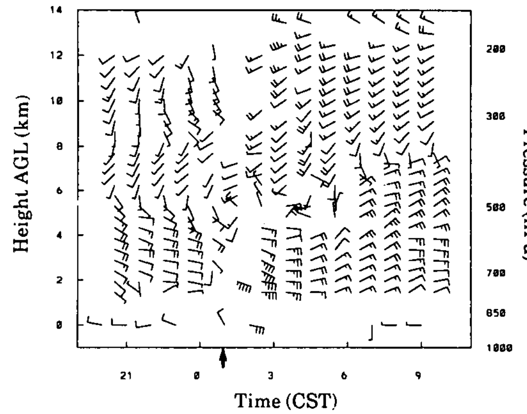

Fig. 6 Vertical motion field associated with the squall analysed using 30-minute averages. The arrival of the squall is marked by the arrow.

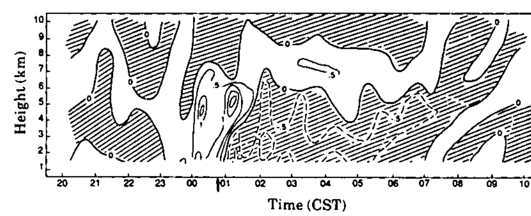

Fig. 7 Sample of the radar spectra from the vertical beam averaged from 0500 to 0600 on 11 November 1990. Positive velocities are toward the radar (downward).

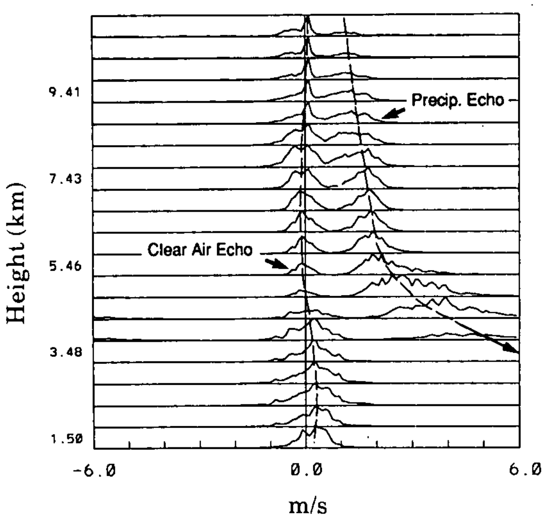

Detailed examination of the radar spectra revealed scatter from snow above the freezing level in the stratiform region (Fig. 7). The maximum height where the snow echo was observed decreased at a rate consistent with the observed fall speed and ended at the rear of the stratiform region. There was also a significant bright band signal observed in the stratiform region. A precipitation signal below the bright band was also observed. The vertical circulations and cloud microphysics revealed by these observations are consistent with theoretical and conceptual models of tropical squall lines (e.g. Ruttledge 1986). This case study provides a brief example of the use of profiler and radar data as diagnostics for the analysis of significant weather events.

Concluding comments

Wind profilers are already having a significant impact, and this will definitely increase as large networks of systems are deployed. These radars are particularly useful for monitoring mesoscale features such as fronts and squall lines, as well as supplying wind data for synoptic analyses. However, these observing platforms are mainly limited to continental areas, although the Aeronomy Laboratory of NOAA is installing a chain of radars in the equatorial Pacific and there is a proposal to have profiler/RASS systems on ships as part of TOGA/COARE. There remains the need for wind measurements over much of the globe. These will require satellite observations, for example scatterometer measurements of surface wind and Doppler lidar observations of upper air winds in clear conditions. Another key problem is humidity sounding. Although ground-based microwave radiometers can accurately measure the column-integrated water vapour and liquid water, height information is required. No good all-weather remote sensing system has been built as yet, although radiometers using the 90 and 183 GHz bands may provide some height information for water vapour.

Acknowledgments

Numerous discussions with T.D. Keenan, K.P. Moran, R.G. Strauch and R.A. Vincent are greatly appreciated.

References

Atlas, D. 1962. Indirect probing techniques. *Bull. Am. met. Soc.*, *43*, 457–66.

Balsley, B.B. 1981. The MST technique—a review. *J. Atmos. Terr. Phys.*, *43*, 495–509.

Beckman, S.K. 1990. Operational use of profiler data and satellite imagery to evaluate the NMC numerical models in predicting heavy snow. *Weath. forecasting*, *5*, 259–77.

Bonino, G., Lombardini, P.P., Longhetto, A. and Trivero, P. 1981. Radio acoustic measurements of a fog-capping thermal inversion. *Nature*, *290*, 121–3.

Ecklund, W.L., Clark, D.A. and Balsley, B.B. 1988. A UHF wind profiler for the boundary layer and initial results. *J. Atmos. Oceanic Tech.*, *5*, 432–41.

Elsberry, R.L. 1990. International experiments to study tropical cyclones in the western north Pacific. *Bull. Am. met. Soc.*, *71*, 1305–16.

Fetter, R.W. 1961. The EMAC probe—a new concept for atmospheric sounding by radar, *Proc. 9th Weather Radar Conference*, Kansas City, 385–90.

Fritts, D.C., Tsuda, T., VanZandt, T.E., Smith, S.A., Sato, T., Fukao, S. and Kato, S. 1990. Studies of velocity fluctations in the lower atmosphere using the MU radar. Part II: Momentum fluxes and energy densities. *J. Atmos. Sci.*, *47*, 51–66.

Fukao, S., Sato, T., Kato, S., Wakasugi, K. and Makihara, T. 1985. The MU radar with an active phased array system 1: Antenna and power amplifiers, *Radio Sci.*, *20*, 1155–68.

Gage, K.S., McAfee, J.R., Collins, W.G., Soderman, D., Bottger, H., Radford, A. and Balsley, B. 1988. A comparison of winds observed at Christmas Island using a wind-profiling Doppler radar with NMC and ECMWF analyses, *Bull. Am. met. Soc.*, *69*, 1041–6.

Gal-Chen, T. 1988. A theory for the retrievals of virtual temperature from remote measurements of horizontal winds and thermal radiation. *Mon. Weath. Rev.*, *116*, 1302–19.

Gossard, E.E. 1988. Measuring drop size distributions in clouds with clear air sensing Doppler radar. *J. Atmos. Ocean. Tech.*, *5*, 640–9.

Keenan, T.D. and Carbone, R.E. 1989. *A preliminary morphology of convective systems in tropical northern Australia. 24th Conf. Radar Meteorology*, Amer. Met. Soc., Tallahassee, Fl, 640–4.

Keyser, D. and Shapiro, M.A. 1986. A review of the structure and dynamics of upper-level frontal zones. *Mon. Weath. Rev.*, *114*, 452–99.

Kuo, Y.-H. and Guo, Y.-R. 1989. Dynamic initialisation using observations from a hypothetical network of profilers. *Mon. Weath. Rev.*, *117*, 1975–98.

Kuo, Y-H., Gill, D.O. and Cheng, L. 1987. Retrieving temperature and geopotential fields from a network of wind profiler observations. *Mon. Weath. Rev.*, *115*, 3146–65.

Larsen, M.F. and Rottger, J. 1982. VHF and UHF Doppler radars as tools for synoptic research. *Bull. Am. met. Soc.*, *63*, 996–1008.

Matuura, N., Masuda, Y., Inuki, H., Kato, S., Fukao, S., Sato, T. and Tsuda, T. 1985. Radio acoustic measurement of temperature profile in the troposphere and lower stratosphere. *Nature*, *333*, 426–8.

May, P.T. 1990. Spaced antenna versus Doppler radars: A comparison of techniques revisited. *Radio Sci.*, *25*, 1111–19.

May, P.T., Moran, K.P. and Strauch, R.G. 1989. The accuracy of RASS temperature measurements. *Jnl. appl. Met.*, *28*, 1329–35.

May, P.T., Strauch R.G. and Moran, K.P. 1988. The altitude coverage of temperature measurements using RASS with wind profiler radars. *Geophys. Res. Lett.*, *15*, 1381–4.

May, P.T., Strauch, R.G., Moran, K.P. and Ecklund, W.L. 1990a. Temperature sounding by RASS with wind profiler radars: a preliminary study. *IEEE Trans. Geosci. Remote Sens.*, *28*, 19–28.

May, P.T., Wilson, K.J. and Ryan, B.F. 1990b. VHF radar studies of cold fronts traversing southern Australia. *Beitrage Atmos. Physik*, *63*, 257–69.

Moran, K.P., Strauch, R.G., Earnshaw, K.B., Merritt, D.A., Weber, B.L. and Wuertz, D.B. 1989. *Lower tropospheric profiler. 24th Conf. Radar Meteorology*, Tallahassee, Fl, 728–31.

Nieman, P.J. and Shapiro, M.A. 1989. Retrieving horizontal temperature gradients and advections from single station wind profiler observations. *Weath. forecasting*, *4*, 222–33.

Nieman, P.J., May, P.T., Stankov, B.B. and Shapiro, M.A. 1991. Radio Acoustic Sounding System observations of an arctic front. *Jnl. appl. Met.*, *6*, 881–92.

North, E.M., Peterson, A.M. and Parry, H.D. 1973. RASS, a remote sensing system for measuring low-level temperature profiles. *Bull. Am. met. Soc.*, *54*, 912–19.

Peters, G., Timmerman, H. and Hinzpeter, H. 1983. Temperature sounding in the atmospheric boundary layer by RASS-system analysis and results. *Int. J. Remote Sens.*, *4*, 49–63.

Reeder, M.J. and Smith, R.K. 1987. A study of frontal dynamics with application to the Australian summertime cool change. *J. Atmos. Sci.*, *44*, 687–705.

Rottger, J. 1979. VHF radar observations of a frontal passage. *Jnl appl. Met.*, *18*, 85–91.

Ruttledge, S.A. 1986. A diagnostic modelling study of the stratiform region associated with a tropical squall line. *J. Atmos. Sci.* *43*, 1356–77.

Ryan, B.F. and Wilson, K.J. 1985. The Australian summertime cool change Part III, Subsynoptic and mesoscale model. *Mon. Weath. Rev.*, *113*, 224–40.

Schroeder, J.A., Westwater, E.R., May, P.T. and McMillin, L.M. 1991. Prospects for temperature sounding with satellite and ground-based RASS measurements. *J. Atmos. Ocean. Tech.*, *8*, 506–13.

Shapiro, M.A., Hample, T. and van de Kamp, D.W. 1984. Radar wind profiler observations of fronts and jet streams. *Mon. Weath. Rev.*, *112*, 1263–6.

Strauch, R.G., Merritt, D.A., Moran, K.P., Earnshaw, K.B. and van de Kamp, D. 1984. The Colorado wind profiling network. *J. Atmos. Ocean. Tech.*, *1*, 37–49.

Vincent, R.A., May, P.T., Hocking, W.K., Elford, W.G., Candy, B. and Briggs, B.H. 1987. First results with the Adelaide VHF radar: spaced antenna studies of tropospheric winds. *J. Atmos. Terr. Phys.*, *49*, 353–66.

Wakasugi, K., Balsley, B.B. and Clark, T.L. 1987. The VHF Doppler radar as a tool for cloud and precipitation studies. *J. Atmos. Ocean. Tech.*, *4*, 273–80.

Weber, B.L. and Wuertz, D.A. 1990. Comparison of rawinsonde and wind profiler radar measurements. *J. Atmos. Ocean. Tech.*, *7*, 157–74.

Woodman, R.F. and Guillen, A. 1973. Radar observations of wind and turbulence in the stratosphere and lower mesosphere. *J. Atmos. Sci.*, *31*, 493–505.

Wuertz, D., Weber, B., Strauch, R.G., Frisch, A.S. Little, G., Merritt, D.A., Moran, K.P. and Welsh, D.C. 1988. Effects of precipitation on UHF wind profiler measurements. *J. Atmos. Ocean. Tech.*, *5*, 450–65.

Zamora, R.J., Shapiro, M.A. and Doswell, C.A. III. 1987. The diagnosis of upper tropospheric divergence and ageostrophic wind using profiler wind observations. *Mon. Weath. Rev.*, *115*, 871–84.